Single-ended Coherent Receivers: From DC-coupled to AC-coupled Photodetectors

Son Thai Le[1,*]

[1]Nubis Communications, NJ, USA, son.le@nubis-communications.com
[*]This work was done at Nokia Bell Labs, NJ, USA

Abstract: We review the concept of single-ended coherent receivers and discuss how LO power and signal power can be accurately estimated when AC-coupled photodetectors are used instead of DC-coupled photodetectors.

OCIS codes: (060.2330) Fiber optics communications; (060.1660) Coherent communications.

1. Introduction

Commercial coherent transceivers (CR) [1] utilize balanced PD (BPDs) with high single-port rejection ratio (SPRR) to mitigate the signal-signal beat interference (SSBI) due to the square-law detection process. In practical implementations, SPRR degrades at high frequencies due to the imbalances of the optical hybrid, RF circuity in both amplitude and skew and the imbalance of the two single-ended PDs within a BPD in responsivities, polarization dependencies and frequency responses [2]. This creates a serious challenge for ultrahigh symbol rate systems (beyond 100 Gbaud). One interesting approach for overcoming this problem while simultaneously reducing the hardware complexity is to replace BPDs by single-ended PDs in a so-called single-ended coherent receiver (SER) [3-6]. It has been demonstrated in [3] that the SSBI in SER can be effectively compensated using low-complexity DSP algorithms. With these techniques, SER has shown compatible performance to the conventional balanced CR for a 90-Gbaud system [4]. For 200-Gbaud transmission, where the imbalance of balanced CR becomes severe, SER even provides performance benefit at a low LO power [5].

On the other hand, SSBI removal techniques in SER require knowledge of the DC components, e. g. the LO and signal powers [3]. Because of that, all previous demonstrations of SERs simply utilized DC-coupled PDs [3-6]. However, the DC component at the output of the PD causes unwanted bias, leading to higher noise and even overloading in subsequent circuits such as transimpedance amplifiers (TIA) and the under-utilization of the ADC resolution. Using AC-coupled PDs eliminate these problems, however, a DSP algorithm for DC components recovery is required for effective SSBI removal [3].

In this paper, we review the concept of SER and discuss an accurate technique for estimating both the LO and signal powers in a SER without using a preamble or prior knowledge of the LO to signal power ratio (LOSPR). This technique relies on the signal statistic and is suitable for systems with reach longer than 20 km.

2. AC-coupled SER and DC-components recovery technique

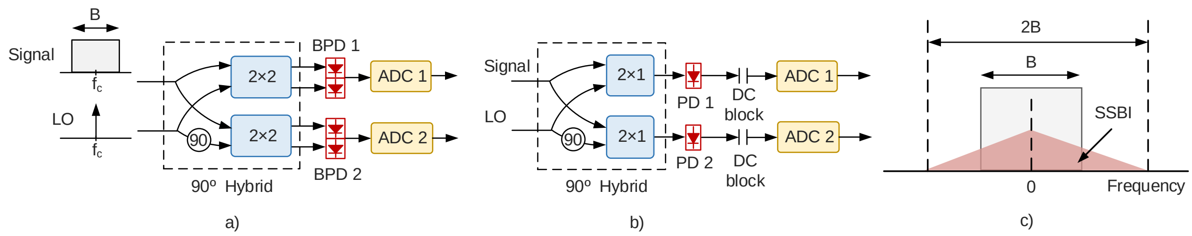

Fig. 1a) – Balanced CR in a single polarization; b) – AC-coupled SER in a single polarization; c) – SSBI in an AC-coupled SER

The block diagram of an AC-coupled SER in single polarization is shown in Fig. 1b in comparison with its BR counterpart shown in Fig. 1a. For simplicity, let us assume that the received complex optical signal is $E(t) = \sqrt{2}(I(t) + jQ(t))$ and the LO is $E_{LO}(t) = \sqrt{2}A$, where A is a positive number. By assuming the PDs are ideal (ideal square-law detectors), the detected analog signals at the outputs of the two single-ended AC-coupled PDs can be written as [3]:

$$\begin{cases} R_1(t) = I(t)^2 + Q(t)^2 + 2AI(t) - P \\ R_2(t) = I(t)^2 + Q(t)^2 + 2AQ(t) - P \end{cases} \quad (1)$$

where $P = \boldsymbol{E}\{I(t)^2 + Q(t)^2\}$ is the average power of the received optical signal. One can note that the detected signals include both the useful detection terms, $2AI(t)$ and $2AQ(t)$, and the SSBI $(I(t)^2 + Q(t)^2)$ which is proportional to the detected optical signal intensity.

In order to recover the DC components, A^2 and P, directly from Eq. 1, we assume that $I(t)$ and $Q(t)$ are zero-mean and statistically independent, e. g $\boldsymbol{E}\{I(t)\} = \boldsymbol{E}\{Q(t)\} = \boldsymbol{E}\{I(t) \cdot Q(t)\} = 0$. One can then easily verify that: $G_1 = \boldsymbol{E}\left\{\left(R_1(t) - R_2(t)\right)^2\right\} = \boldsymbol{4}A^2P$. Next, we calculate:

$$G_2 = \boldsymbol{E}\left\{\left(R_1(t)\right)^2\right\} + \boldsymbol{E}\left\{\left(R_2(t)\right)^2\right\} = 2\boldsymbol{E}\{(I(t)^2 + Q(t)^2)^2\} - 2P^2 + 4A^2P \quad (2)$$

Let us denote: $G_3 = \boldsymbol{E}\{(I(t)^2 + Q(t)^2)^2\}/P^2$, we then have: $G_2 = 2G_3P^2 - 2P^2 + 4A^2P$ and:

$$P = \sqrt{\frac{G_2 - G_1}{2G_3 - 2}} = \sqrt{\gamma(G_2 - G_1)}, \text{ and } A^2 = \frac{G_1}{4\sqrt{\gamma(G_2 - G_1)}}, \quad (3)$$

where $\gamma = 1/(2G_3 - 2)$. Eq. 3 indicates that if γ is known, both the LO power (A^2) and signal power (P) can be determined. For high symbol rate transmission, with sufficient dispersion, both $I(t)$ and $Q(t)$ at the Rx can be statistically modelled by a Gaussian distribution. As a result, $I(t)^2 + Q(t)^2$ has a Chi-squared distribution [7]. Fig. 2a shows the probability density function (PDF) of $2(I(t)^2 + Q(t)^2)/P^2$ for 100-Gbaud 16-QAM signal with 5% RRC pulse shaping at the B2B and over 20-km of standard single-mode transmission at 1550 nm. One can see that even after only 20-km of transmission, $2(I(t)^2 + Q(t)^2)/P^2$ converges to a Chi-squared distribution. For a Chi-squared distribution, one can verify that:

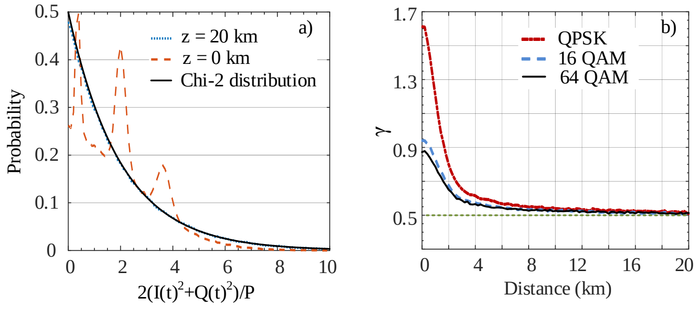

Fig. 2a) – PDF of $2(I(t)^2 + Q(t)^2)/P^2$ for 100 Gbaud 16 QAM signal; b) – γ as function of distance for 100 Gbaud signal with QPSK, 16-QAM and 64-QAM

$$G_3 = \boldsymbol{E}\{(I(t)^2 + Q(t)^2)^2\}/P^2 = 2 \text{ , and thus } \gamma = 1/(2G_3 - 2) = 0.5$$

Figure 2b depicts the numerical simulation for γ which shows that γ is generally dependent on the signal format, baudrate and also the distance. In the B2B case, γ is much higher for QPSK than for 16-QAM and 64-QAM. However, after only ~ 20-km, γ converges to 0.5 for all considered formats. As a result, both LO and signal powers can be estimated using Eq. 3 by simply substituting $\gamma = 0.5$ without the need for a training sequence and prior knowledge of the LOSPR.

To discuss the accuracy of the abovementioned algorithm, we define two estimation errors (in %) as $e_A(L) = 100\%(A_{est} - A)/A$ and $e_{DC}(L) = 100\%\left((A_{est}^2 + P_{est}) - (A^2 + P)\right)/(A^2 + P)$, where L is the number of samples (at 2sps) taken into calculation. Figure 3 shows the worst-case scenarios for $e_A(L)$ and $e_{DC}(L)$ considering 1000 random 100-Gbaud 16-QAM sequences. As expected, the presented technique accuracy increases with L. At $L = 10^6$, $Max\{|e_A(L)|\} < 5\%$ for all considered values of LOSPR (from 0 dB to 10 dB). At $L = 10^7$, $Max\{|e_A(L)|\}$ further drops below 2%. One can also note that reducing the LOSPR significantly increases the estimation accuracy. This is because the presented technique is based on the independent statistical properties of $I(t)$ and $Q(t)$ and their contributions for the estimation accuracy increase when the LOSPR is reduced. For a similar reason, the estimation accuracy also increases when the OSNR decreases because a larger ASE noise makes $I(t)$ and $Q(t)$ more statistically independent and better approximated by Gaussian distributions. Overall,

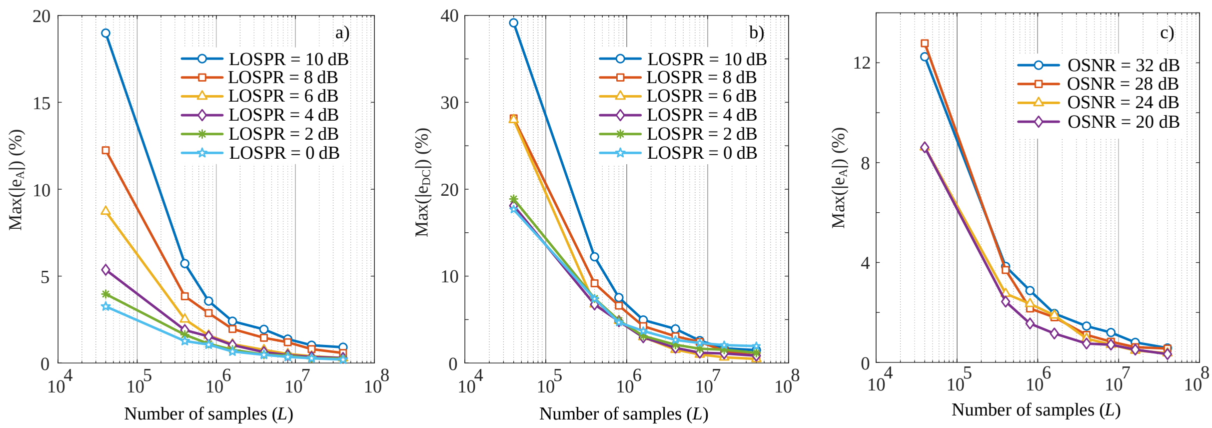

Fig. 3a, 3b) – Max $|e_A(L)|$ and Max $|e_{DC}(L)|$ as function of L for various LOSPR values at OSNR of 32 dB; c) – Max $|e_A(L)|$ as function of L for various OSNR values at LOSPR of 8-dB; The signal is 100-Gbaud 16-QAM with 5% RRC over 20km

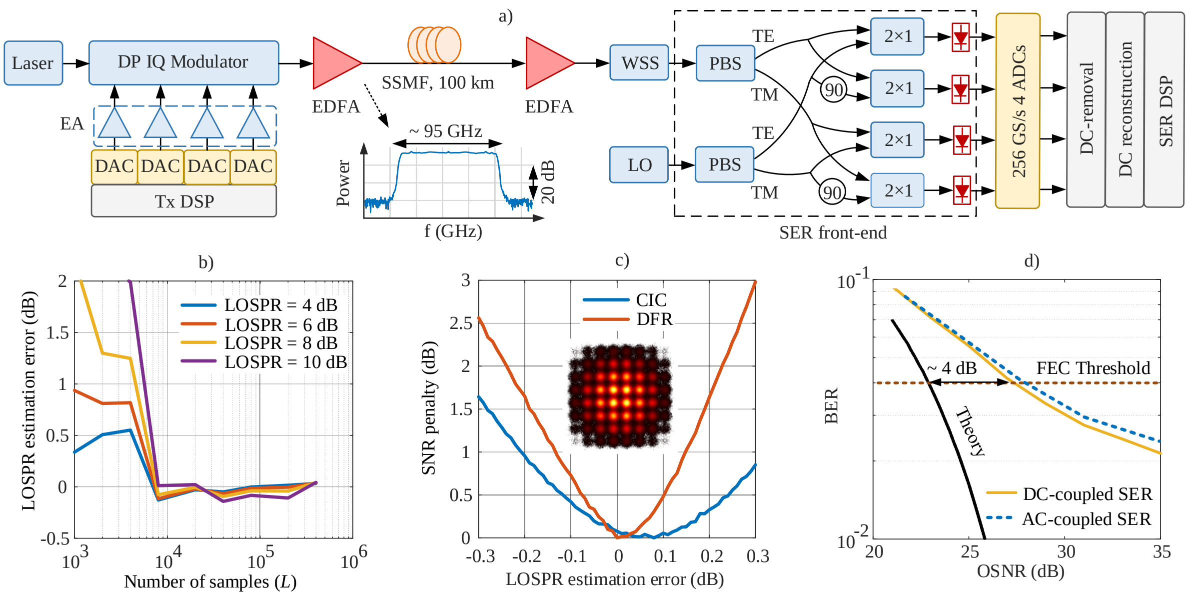

Fig. 4a) Experimental setup for 90-Gbaud PCS 64-QAM transmission over 100-km using a self-calibrated SER; PBS – polarization beam splitter, WSS – wavelength selective switch; b) – LOSPR estimation errors; c) – SNR penalty versus LOSPR estimation error for SER with CIC and DFR techniques; d) – Sensitivities comparison of the considered DC-coupled and AC-coupled SERs for LOSPR = 10 dB

Fig. 3 shows that if L is large enough, the presented technique can provide an excellent performance regardless of OSNR and LOSPR values.

3. Experimental verification

We set up a 90-Gbaud probabilistically constellation shaped (PCS) 64-QAM (with an entropy of 5.6 bits/symbol/polarization) transmission over 100 km of SSMF as depicted in Fig. 4a. The detail of this experimental setup can be found in [3, 4]. In this setup, we used 4 DC-coupled PDs for signal detection. To emulate an AC-coupled SER, the DC components of the 4 received signals from the real-time scopes were removed. Next, the AC-coupled signals were fed to a DC component reconstruction block which estimated both the signal power and LO power. Then SER DSP was performed using either the direct field reconstruction (DFR) or clipped iterative SSBI cancellation techniques (CIC) [3] with 4 iterations and a clipping ratio of 9 dB.

Figure 4b shows the LOSPR estimation error (in dB) as a function of L for LOSPR values from 4 dB to 10 dB. One can note that at $L = 10^4$ a remarkable accuracy in LOSPR of below 0.1 dB could already be achieved. We note that 0.1 dB is already within the accuracy of the optical power meter used for the actual LOSPR measurement. Apparently, using PCS signals increases the estimation accuracy because PCS signals are better approximated by Gaussian distributions compared with conventional QAM. Fig. 4c shows the impact of an LOSPR estimation error on the effective SNR. One can see that even 0.1 dB of LOSPR estimation error can lead to 0.5 dB degradation in SNR for the DFR technique. For CIC technique, the tolerance to DC reconstruction error is better and overestimating the LOSPR leads to a smaller SNR penalty compared to underestimating the LOSPR. Nevertheless, the high sensitivity of SNR on the LOSPR value clearly indicates the importance of having an accurate LOSPR estimation or measurement method in SER.

Figure 4c shows that when the LOSPR is accurately estimated, there should be negligible performance difference between DC-coupled SER and AC-coupled SER. In our experiment, we emulated an AC-coupled SER from a DC-coupled SER which actually suffers from higher quantization noise. As a result, we expect that AC-coupled SER to outperform DC-coupled SER in practical implementations.

4. Conclusion

With an accurate DC-components reconstruction technique, an AC-coupled SER shows no performance penalty compared to its DC-coupled SER counterpart and thus it can be an attractive candidate for DCI, metro and campus connection applications.

5. References

1. K. Kikuchi, "Fundamentals of Coherent Optical Fiber Communications," in JLT, vol. 34, no. 1, pp. 157-179, Jan.1, 2016
2. Yves Painchaud et al "Performance of balanced detection in a coherent receiver," Opt. Express 17, 3659-3672 (2009)
3. S. T. Le, V. Aref and J. H. Cho, "Single-Ended Coherent Receiver", in Journal of Lightwave Technology, 2022
4. S. T. Le et al, "882 Gbps Transmission over 100 km of SSMF using a Self-Calibrated Single-ended Coherent Receiver" OFC 2021
5. S. T. Le, V. Aref and X. Chen, "2 Tb/s Single-ended Coherent Receiver," ECOC 2021, pp. 1-4
6. T. M. Hoang et al., "Transmission of 344 Gb/s 16-QAM Using a Simplified Coherent Receiver Based on Single-Ended Detection," IEEE Photonics Journal, vol. 8, no. 3, pp. 1-8, June 2016.
7. https://en.wikipedia.org/wiki/Chi-squared_distribution